# Role of SCFAs for fimbrillin-dependent biofilm formation of *Actinomyces oris* and regulation of *SMU.940* for dextran-dependent aggregation and biofilm formation in *Streptococcus mutans*

# *Actinomyces oris* の fimbrillin 依存的なバイオフィルム形成における SCFAs の役割と *Streptococcus mutans* のデキストラン依存的な凝集およびバイオフィルム形成における *SMU.940* 遺伝子による制御

鈴木　到

日本大学大学院松戸歯学研究科 小児歯科学専攻

(指導: 清水 武彦 教授)

## 1. Abstract

*Actinomyces oris* expresses type 1 and 2 fimbriae on the cell surface. Type 2 fimbriae mediate co-aggregation and biofilm formation and are composed of the shaft fimbrillin FimA and the tip fimbrillin FimB. Short-chain fatty acids (SCFAs) are metabolic products of oral bacteria, but the effects of exogenous SCFAs on FimA-dependent biofilm formation are poorly understood. Two types of biofilm formation assays were performed using *A. oris* MG1 or MG1.Δ*fmA* to observe the effects of SCFAs on FimA-dependent biofilm formation in 96-well and 6-well micro titer plates and a flow cell system. SCFAs did not induce 6- and 16-h biofilm formation of *A. oris* MG1 and MG1.Δ*fmA* in saliva-coated 96-well and six-well microtiter plates in which metabolites produced during growth were not excluded. However, 6.25 mM butyric acid and 3.125 mM propionic acid induced FimA-dependent biofilm formation and cell death in a flow cell system in which metabolites produced during growth were excluded. Metabolites produced during growth may lead to disturbing effects of SCFAs on the biofilm formation. The pure effects of SCFAs on biofilm formation were induction of FimA-dependent biofilm formation, but the stress responses from dead cells may regulate its effects. Therefore, SCFA may play a key role in *A. oris* biofilm formation. The oral bacterium *Streptococcus mutans* is the principal agent in the development of dental caries. Biofilm formation by *S. mutans* requires bacterial attachment, aggregation, and glucan formation on the tooth surface

under sucrose supplementation conditions. Previous microarray analysis of clinical strains identified 74 genes in *S. mutans* that were related to biofilm morphology; however, the roles of almost all of these genes in biofilm formation are poorly understood. The inactivation of the *SMU.940* gene of *S. mutans* UA159 promoted rapid dextran-dependent aggregation and biofilm formation in tryptic soy broth without dextrose (TSB) with 0.25% glucose and slightly reduced biofilm formation in TSB with 0.25% sucrose. GbpC is known to be involved in the dextran-dependent aggregation of *S. mutans*. The *gbpC* mutation completely abolished the dextran-dependent aggregation of the *SMU.940* mutant. These findings suggest that *SMU.940* contributes to the regulation of dextran-dependent aggregation and biofilm formation.

Keywords: biofilm; *Actinomyces oris*; SCFAs; aggregation; *Streptococcus mutans*

## 2. Introduction

The initial attachment of bacteria plays an important role in colonization and interactions with other bacteria on the tooth surface during oral biofilm formation in the human oral cavity [1–4]. *Actinomyces oris*, formerly called *Actinomyces naeslundii* genospecies 2 [5, 6], is a well-known early colonizer that interacts with other bacteria in the oral cavity [6, 7]. Fructosyltransferases (FTFs) of *A. naeslundii* synthesize levan, which contributes to cell-cell communication in biofilm formation, but not initial attachment [8]. Levan is an important factor that induces biological activities. *Actinomyces* spp. aggregate with *streptococci* spp. during the progression of dental caries [9] and contribute to periodontal diseases in the presence of levan [9–11]. *A. oris* induces co-aggregation with *Streptococcus gordonii* and *Streptococcus sanguinis* as early colonizers and *Fusobacterium nucleatum* as middle colonizers in oral biofilms [1].

*Actinomyces* binds to proline-rich proteins (PRPs) and statherin, which is a phosphate-containing protein in saliva [1]. *A. oris* expresses two types of important fimbriae on its cell surface. Type 1 fimbriae are constructed of shaft fimbrillin FimP and tip fimbrillin FimQ. Type 2 fimbriae are constructed of shaft fimbrillin FimA and tip fimbrillin FimB [12]. Type 1 fimbriae mediate attachment to PRPs on the tooth surface [13], and type 2 fimbriae mediate co-aggregation and biofilm formation [14]. Type 2 fimbriae of *A. oris* are necessary for the recognition of streptococci, which express polysaccharide receptors [15, 16].

Short-chain fatty acids (SCFAs) are secreted from numerous oral bacteria, including *Porphyromonas gingivalis* and *Fusobacterium nucleatum* [17, 18]. In healthy human volunteers, the concentrations of acetic acid, lactic acid, propionic acid, formic acid, butyric acid and valeric acid were detected in saliva as 6.0 ± 3.5 mM, 1.2 ± 1.9 mM, 1.0 ± 0.8 mM, 0.5 ± 0.5 mM, 0.3 ± 0.4 mM and 0.05 ± 0.2 mM, respectively [19]. High concentrations of butyric acid and propionic acid were mainly detected in periodontal pockets of severe and mild periodontal disease subjects, 2.6 ± 0.4 mM and 0.2 ± 0.04 mM, and 9.5 ± 1.8 mM and 0.8 ± 0.3 mM, respectively [17]. In another report, elevated concentrations of butyric acid (range 4.7–13. 8 mM) and propionic acid (range 87–112 mM) were also detected in dental plaques [20]. According to past report, 6.25 mM butyric acid increased *A. naeslundii* X600 biofilm in 96-well microtiter plates; SDS-PAGE and Western blotting of biofilm cells demonstrated that the heat shock protein GroEL mediated this upregulation [21]. Another report demonstrated that 60 mM butyric acid increased *A. naeslundii* X600 biofilm in a flow cell system and the initial attachment of *A. naeslundii* X600 cells in six-well culture plates; GroEL also mediated this phenomenon [8]. These reports suggest that butyric acid induces the cell status potential for biofilm formation. However, the relationship between SCFAs and fimbrillin-dependent biofilm formation of *A. oris* is poorly understood.

The present study performed biofilm formation assays to elucidate the relationship

between fimbriae and SCFAs. We clearly demonstrated that SCFAs did not induce biofilm formation of *A. oris* MG1 and MG1.Δ*fimA* in human saliva-coated 96-well and 6-well microtiter plates. However, butyric acid and propionic acid induced FimA-dependent biofilm formation in a flow cell system. These results in different assay types provide new mechanisms of fimbrillin-dependent biofilm formation stimulated with SCFAs in *A. oris* and oral bacteria producing SCFAs.

*Streptococcus mutans* is a Gram-positive oral bacterium that is one of the causative agents associated with dental caries [37, 38]. The pathogenic activities of *S. mutans* are related to the high capacity for producing and tolerating acids, the possession of high-affinity systems for the assimilation of various carbohydrate sources, and the formation of sticky biofilms. Bacterial attachment, aggregation and the formation of biofilm on the tooth surface are important steps in the progression of dental caries. Water-insoluble glucan synthesized using GtfB (GTF-I)- and GtfC (GTF-SI)-glucosyltransferases, which are encoded by *gtfB* and *gtfC*, promotes the adhesion to tooth surfaces and the aggregation of bacterial cells within the biofilm under sucrose supplementation conditions in *S. mutans* [39-41]. Surface-associated glucan-binding proteins (Gbps) also mediate the aggregation, biofilm formation, and adherence to glucan, thereby promoting plaque formation and contributing to the cariogenicity of *S. mutans* [42, 43]. GbpC, which is a cell-associated protein, is believed to be the most important Gbp in *S. mutans*

as it directly contributes to cariogenicity [44, 45]. GbpC-defective strains have a reduced capacity to form biofilms, and the structure of the biofilms formed is markedly different from that of the wild-type [42]. GbpC also promotes dextran-dependent aggregation in vitro under stress conditions [46, 47]. GbpC may interact with the dextran that is produced by early colonizer species or that produced in response to stresses in the oral cavity, resulting in the aggregation of bacteria [48].

The various mechanisms underlying biofilm formation may be beneficial for survival and persistence in the oral ecosystem. Recently, the gene expression in flow cell biofilms of two clinical isolates of *S. mutans* serotype c, ie high-biofilm-forming FSC-3 and low-biofilm-forming FSC-4 were analyzed using a microarray analysis [49]. Differential expression of 74 genes in the biofilms of the two strains were found. Microarray analyses can be used to identify novel biofilm-associated factors; however, the roles of most identified genes are not understood. Of the 21 genes that were up-regulated in FSC-3 relative to FSC-4, 8 genes were identified as competence-stimulating peptide (CSP)-dependent genes, and only *SMU.940*, which presumably encodes a hemolysin III-related protein, played a role in the regulation of the rapid aggregation.

In this study, CSP-dependent genes, *SMU.940*, played a role in the regulation of the rapid aggregation was focused. The role of *SMU.940* in biofilm formation and cell aggregation were

investigated.

## 3. Materials and Methods

### 3.1. Bacterial strains and culture conditions

*Actinomyces oris* MG1 and its derivatives were grown in brain-heart infusion (BHI) broth (BD Diagnostics, Sparks, MD, USA) at 37 °C in a 5% $CO_2$ aerobic atmosphere (AnaeroPack; Mitsubishi Gas Chemical Co., Tokyo, Japan). The fimbriae deletion mutant *A. oris* MG1.Δ*fimA* [13, 14] was provided by Prof. Hung Ton-That, University of Texas Health Science Center, Houston, Texas. Tryptic soy broth without dextrose (TSB; Difco Laboratories, Detroit, MI, USA) supplemented with 0.25% sucrose (TSBs) with or without different concentrations (3.125, 6.25, 7.5, 10, 15, 20, 30 or 60 mM) of SCFAs (acetic, butyric, formic, lactic, propionic or valeric acids) was prepared for each experiment.

The *S. mutans* laboratory strain UA159 and its derivatives were maintained and grown in BHI broth at 37°C in a 5% $CO_2$ aerobic atmosphere. The *SMU.940* mutant made in our laboratory was used for this study. TSB supplemented with 0.25% glucose (TSBg) or TSBs was used for the assessment of the biofilm formation and aggregation.

### 3.2. Human saliva collection

Human whole saliva samples were collected from 3 healthy volunteers (22~27 years old) after stimulation by chewing paraffin gum and pooled into ice-chilled sterile bottle over a period of 5 min. The samples were clarified by centrifugation at 10,000 × g for 10 min at 4 °C. Supernatants were transferred into new sterile tubes and sterilized using a 0.22-μm Millex-GP filter (Merck Millipore; Bedford, MA, USA). Sterilized human saliva was stored at −20 °C until use.

3.3. Biofilm formation assay in 96-well and 6-well plates of *A. oris*

Biofilm formation of *A. oris* was assayed using a previously described method [20]. Before the biofilm formation assay, sterilized human saliva was coated on the well from a 96-well culture plate or on a 6-well culture plate sterilized cover glass placed at 4 °C for 1 h. After coating, the wells were washed using sterilized phosphate-buffered saline (PBS, pH 7.4). *A. oris* MG1 and FimA deletion mutants were diluted with flesh TSBs, and bacterial cells were adjusted to an optical density of 0.4 at 600 nm. To analyze the quantity of biofilm formation, 20 μL of bacterial suspensions were mixed with 180 μL of TSBs with or without SCFAs. The mixture was added to human saliva-coated or non-coated 96-well plates and incubated at 37 °C for 6 or 16 h. These concentrations of SCFAs were applied in biofilm formation assay to observe largely the activities of SCFAs. To analyze the quality of biofilm formation, 200 μL cell

suspensions were mixed with 1800 μL of TSBs with or without SCFAs, and the mixture was added to human saliva-coated cover glass in 6-well culture plates and incubated at 37 °C for 16 h. The 96-well or 6-well culture plates were gently washed using PBS, 2-times and sufficiently dried. Biofilms in 96-well plates were stained with 0.5% safranin for 15 min, washed with distilled water, air-dried, solubilized in a 70% ethanol solution, and quantified at an absorbance of 492 nm. The biofilms in 6-well plates were also stained with the FilmTracer Live/Dead Biofilm Viability kit (Molecular Probes, Inc., Eugene, OR, USA), which was applied to the biofilms at final concentrations of 5 μM SYTO9 and 30 μM propidium iodide, respectively, and observed using Confocal Laser Scanning Microscope (CLSM). Biofilms were incubated with the dyes at room temperature for 20–40 min and imaged using a confocal microscope (LSM700 Meta NLO CLSM, Carl Zeiss Inc., Thornwood, NY, USA). Confocal images were photographed with a 63× immersion oil objective in the biofilm on the cover glass in the 6-well culture plates. Confocal microscopy acquisition parameters (pinhole, detector and amplifier gain, amplifier offset filters) were set using reference samples and were kept constant in the acquisition of all the remaining images. CLSM images were acquired using an argon laser at 488 and a HeNe-G laser at 555 nm. The independent and triplicate experiments were performed 3 times. Three fields of view were analyzed in each sample. Confocal images of biofilm formation were visually observed using ZEN analysis software (Carl Zeiss, Oberkochen,

Germany).

3.4. Flow cell biofilm formation assay of *A. oris*

Flow cell biofilm formation of *A. oris* was assayed using the method of Motegi et al [22]. Briefly, *A. oris* MG1 and MG1.Δ*fimA* were diluted with flesh TSBs, and bacterial cells were adjusted to an optical density of 0.4 at 600 nm. Cell suspensions were inoculated into chambers of a three-channel flow cell system (Stoval Howcell; Stovall Life Science Inc., Greensboro, NC) and incubated at 37 °C for 3 h. TSBs with or without 6.25 or 60 mM butyric acid and 3.125 or 6.25 mM propionic acid were pumped through the flow cells at a constant rate of 3 mL/h for 48 h using a peristaltic pump (Ismatec; IDEX Corp-Glattbrugg-Zürich, Switzerland). Appropriate concentrations were selected from the results in the 96-well culture plates and from references [8, 21] and applied to the flow cell assay. Non-attached cells were removed via washing with distilled water. Confocal images were photographed with a 63× immersion oil objective. Confocal microscopy acquisition parameters (pinhole, detector and amplifier gain, amplifier offset filters) were set using reference samples and were kept constant in the acquisition of all the remaining images. CLSM images were acquired using an argon laser at 488 and a HeNe-G laser at 555 nm. The independent experiments were performed 3 times. Three fields of view were analyzed in each sample. Confocal images of biofilm formation were visually observed

using ZEN analysis software. To calculate live and dead cell total areas, the images of the flow cell biofilm cells were re-analyzed with ImageJ 1.48 software.

### 3.5. Biofilm formation assay of *S. mutans*

Biofilms from each strain were developed in 96-well polystyrene microtiter plates (Sumitomo Bakelite, Tokyo, Japan). The biofilm formation assay was performed as previously described [49]. Wells containing 180 μL of TSB with 0.25% glucose or sucrose were inoculated with 20 μL of the cell culture ($OD_{600}$ = 0.4). The plates were then incubated at 37°C with 5% $CO_2$ for 8 h to measure early biofilm formation because early aggregation has been observed in the *SMU.940* mutant, which is a different phenotype from that of wild-type and other mutants. After the incubation, the planktonic cells were removed by washing with distilled water, and the adherent cells were stained with 0.25% safranin for 15 min. The biofilms were solubilized in a 70% ethanol solution and quantified by measuring the absorbance of the stained biofilms at 492 nm.

### 3.6. Aggregation assay of *S. mutans*

The aggregation assay was performed using the previously described methods [46] with slight modifications under the following culture conditions: parental, *SMU.940* mutant, *gbpC*

mutant, and *SMU.940-gbpC* double mutant cultures were grown to mid-log phase in TSB with 0.25% glucose or overnight in TSB with 0.25% glucose and 4% ethanol. The cultures were incubated at 37°C with 5% $CO_2$. After the incubation, the cultures were centrifuged for 5 min at 2800 g and resuspended in PBS ($OD_{620}$ = 1.0). Then, 100 μg/mL dextran (Sigma-Aldrich, Steinheim, Germany) was added (or not) to the suspensions obtained from the cultures. These samples were incubated at room temperature for 1 h. The turbidity of the suspensions at 0, 5, 10, 15, 20, 25, 30, and 60 min was quantified by measuring the $OD_{620}$.

### 3.7. Statistical analysis

Comparisons of biofilm levels between two groups were performed using Student's t-tests. Statistical significance was defined at p-values <0.05. Additionally, the comparisons of biofilm levels between multiple groups were by one-way analysis of variance and post-hoc Tukey's tests. Data were analyzed using Microsoft Excel and SPSS (IBM SPSS statistics 24, IBM Corporation, Armonk, NY, USA).

## 4. Results

*Actinomyces* spp. interact with salivary components, such as PRPs and statherin, and form biofilms on tooth surfaces [23, 24]. Therefore, the effects of salivary components on six-hour

biofilm formation were examined, and the effects of acetic, butyric, formic, lactic, propionic and valeric acids on *A. oris* biofilm formation were observed in human saliva-coated and non-coated plates. Human saliva components enhanced biofilm formation compared to non-coated wells in the absence of SCFAs and 10 mM butyric acid. However, this was not significant in 0 mM butyric acid, 0 mM propionic acid and 6.25 mM valeric acid (Figure 1). Butyric and valeric acids at 6.25 and 10 mM created equal levels of biofilm formation in the human saliva-coated plates, compared to the no butyric acid control (Figure 1A, C). However, 20 mM and 30 mM butyric acid, compared to the no butyric acid control, significantly inhibited biofilm formation in the human saliva-coated plate. Propionic acid inhibited biofilm formation in human saliva-coated plates at all concentrations, but not in non-coated wells (Figure 1B). Other SCFAs showed similar data to butyric acid, propionic acid and valeric acid (data not shown). Therefore, we concentrated on the effects of butyric acid, propionic acid and valeric acid on the biofilm formation in the following experiments. The effects of FimA mutation and butyric, propionic and valeric acids on *A. oris* biofilm formation in human saliva-coated plates were examined. Mutation of FimA, compared with wild-type MG1, did not inhibit biofilm formation after six hours in all conditions: no SCFAs, butyric acid, propionic acid and valeric acids (Figure 2). Propionic acid enhanced MG1.Δ*fimA* biofilm formation at 10 mM and 20 mM, and valeric acid enhanced MG1.Δ*fimA* biofilm formation at 20 mM compared to the control.

FimA contributes to co-aggregation [25] with streptococci and biofilm formation [26]. Therefore, FimA may play a role during a later stage of biofilm formation. Sixteen-hour biofilm formation assays were observed in conditions with no SCFAs or butyric, propionic and valeric acids in human saliva-coated 96-well microtiter plates to investigate the contribution of FimA at a later stage in biofilm formation. Biofilm formation was significantly lower for MG1.Δ*fimA* than MG1 (Figure 3). Biofilm formation in conditions with butyric and propionic acids at 3.125 and 6.25 mM was significantly lower for MG1.Δ*fimA* than MG1 mutants (Figure 3A, B). Butyric acid at 3.125 and 6.25 mM induced equal levels of biofilm formation for MG1 and controls with no butyric acid. Propionic and valeric acids inhibited MG1 biofilm formation in a dose-dependent manner beginning at 3.125 mM. All SCFAs slightly inhibited MG1.Δ*fimA* biofilm formation in a dose-dependent manner. Taken together, these results indicate that butyric acid exerted different biological activities from other SCFAs. However, butyric acid, compared with controls without SCFAs, did not enhance *A. oris* biofilm formation in 96-well microtiter plates. The biofilm formation level was similar between 3.13 and 6.25 mM butyric acid and controls without butyric acid (Figure 3). However, the quality of biofilm formation may be different between conditions with and without butyric acid. Therefore, live/dead cell staining was performed for MG1 and MG1.Δ*fimA* biofilm formation in conditions with and without butyric acid (Figure 4). To clearly observe biofilm cells in the culture plate by confocal

microscope, the biofilm formation assay was performed on the cover glass coated with human saliva in the six-well culture plates. Live and dead cells were largely observed in MG1 without butyric acid (Figure 4A, B). Merged images revealed that live and dead cells were equally interspersed (Figure 4C). The images of dead cells stimulated with 6.25 mM butyric acid were brighter than images of live cells in biofilm (Figure 4D, E). Merged images indicated that the numbers of dead cells was larger than live cells because an orange color appeared, which indicates that the red staining was mixed more strongly than the green staining (Figure 4F). *A. oris* MG1.Δ*fimA*, compared to MG1, produced a poorer biofilm that included live and dead cells, and 6.25 mM butyric acid did not increase the color of dead cells (Figure 4J-L). Bacteria produce metabolites, including lactic acid, during growth in TSBs. The metabolites mix with SCFAs and may affect *A. oris* biofilm formation. To remove the influence of metabolites produced by fermentation during growth, biofilm formation assays were performed using a flow cell system with *A. oris* MG1 and *A. oris* MG.1Δ*fimA* in 6.25 mM butyric acid (Figure 5). *A. oris* MG1 formed abundant biofilms in TSBs with and without 6.25 mM butyric acid (Figure 5A-C), but the addition of 6.25 mM butyric clearly increased the number of dead cells compared to the control without butyric acid (Figure 5D-F). The biofilm formation of *A. oris* MG1.Δ*fimA* was poor compared to *A. oris* MG1 in TSBs and TSBs with 6.25 mM butyric acid, and 6.25 mM butyric acid did not increase the number of dead cells (Figure 5G-L). Butyric acid

(60 mM) did not induce significant biofilm formation (data not shown). To clarify the roles of dead cells in the biofilm stimulated by butyric acid, X-Z axis images are given in Figure 5C and Figure 5F. Many dead cells attached to the well bottom and largely interacted with live cells in the biofilm induced by butyric acid, but not in the biofilm without butyric acid (Figure 6). Propionic acid (3.125 mM) also promoted dead cells in biofilm formation, but the number of dead cells was fewer than with butyric acid (Figure 7A-L). The biofilm formation of *A. oris* MG1. Δ*fimA* was poor compared to *A. oris* MG1 in TSBs with and without 3.125 mM propionic acid, and 3.125 mM propionic acid did not show clear dead cells (Figure 7G-L). Biofilm formation with 6.25 mM propionic acid was similar to that with 3.125 mM propionic acid (data not shown). To clarify the effects of propionic acid on the biofilm formation and the area of attached and aggregated live and dead cells on the flow cells, ImageJ analysis was performed in the images (Figure 7) from the biofilms stimulated with and without 3.125 mM propionic acid. The area of attached and aggregated cells was significantly increased by propionic acid in *A. oris* MG1, but not in *A. oris* MG1.Δ*fimA* (Figure 8). These results demonstrated that butyric acid and propionic acid induced a FimA-dependent biofilm that included more dead cells and altered the characteristics of the biofilm compared to the control biofilm.

To determine whether the *SMU.940* gene was involved in *S. mutans* early biofilm formation, the *SMU.940* mutant was used and their biofilm-forming abilities were assessed. It

was detected that an approximately two-fold increase in the biomass of the early biofilm formed by the *SMU.940* mutant relative to that formed by the parental strain when grown in TSB medium with 0.25% glucose for 8 h (Figure 9A). In the 0.25% sucrose-supplemented culture, the early biofilm formation of the *SMU.940* mutant in 8 h was slightly reduced compared with that of the parental strain, although the difference was not statistically significant (Figure 9B).

GbpC is known to be involved in the dextran-dependent rapid aggregation of *S. mutans* and is induced by a variety of stress agents, including tetracycline, ethanol, and xylitol [50]. A *gbpC* mutant and a *gbpC-SMU.940* double mutant were prepared to determine the contribution of *gbpC* to the aggregation of the *SMU.940* mutant. It was found that the aggregation of the *SMU.940* mutant was prevented by a mutation in *gbpC* in the TSB medium with glucose (Figure 10A). Furthermore, aggregation assays of all strains in dextran-containing media were performed. It was found that the presence of dextran did not induce rapid aggregation in the parental strain and slightly enhanced the aggregation of the *SMU.940* mutant (Figure 10B) compared with that under the dextran-free condition (Figure 10A). The mutation in *gbpC* inhibited the rapid aggregation of the *SMU.940* double mutant in the presence of dextran (Figure 10B). The addition of ethanol or ethanol and dextran induced rapid aggregation in the parental strain and slightly enhanced the aggregation of the *SMU.940* mutant (Figure 10C, D) compared with that under conditions with and without dextran in the absence of ethanol (Figure

10A, B). However, ethanol and dextran did not induce significant aggregation in the *gbpC* mutants. These results suggest that the aggregation of the *SMU.940* mutant may be affected by *gbpC* expression and stress conditions, such as addition of ethanol to the TSB with 0.25% glucose.

## 5. Discussion

*Actinomyces* spp., including *A. naeslundii* and *A. oris*, are among the most abundant microorganisms present in supra- and sub-gingival dental plaques [4, 27], and these bacteria play a variety of biological activities in the poly-microbial habitats on the tooth surface [1]. Metabolites, such as SCFAs, from oral biofilm bacteria affect the initial attachment, colonization and biofilm formation of *A. naeslundii* [8, 21]. The present study examined the effects of SCFAs on *A. oris* biofilm formation in 96-well microtiter plates coated with human saliva because salivary components interact with *A. oris* [1, 2]. Propionic acid and valeric acid inhibited 16 h biofilm formation at all concentrations. However, butyric acid induced levels of biofilm formation at 3.125 mM and 6.25 mM equal to that of controls and strongly inhibited biofilm formation at concentrations greater than 15 mM. However, more dead cells were observed in the biofilm formation with 6.25 mM butyric acid compared to that of the control. Butyric acid induced dead cell-dependent biofilm formation. This result suggests that damaged

cells adhered and aggregated on solid surfaces coated with human salivary components in TSB with butyric acid.

Butyric and propionic acid concentrations are significantly associated with clinical measures of disease severity (e.g., pocket depth and attachment level), inflammation (e.g., subgingival temperature and the percentage of sites bleeding when probed) and total microbial load (all $p < 0.05$) [17]. The attached and colonized bacterial cells in the present experiment were exposed and received biological stimulation, including stresses with 3.125 mM and 6.25 mM butyric acid, which is physiologically observed in periodontal pockets, for 16 h. Our previous report demonstrated that 6.25 mM butyric acid, 3.125 mM propionic acid and 3.125 mM valeric acid upregulated *A. naeslundii* X600 biofilm formation compared to controls without SCFAs in human saliva-coated 96-well microtiter plates [21]. However, these SCFAs did not increase *A. oris* biofilm formation in this study. Therefore, the susceptibilities of *A. oris*, genospecies 2, to SCFAs are different from *A. naeslundii* X600, which belongs in genospecies 1 [28]. *A. oris* is numerically more successful in oral biofilm formation than *A. naeslundii* (as *A. naeslundii* genospecies 1) [29]. *A. oris* exhibited stronger biofilm formation activities than did *A. naeslundii* x600 in human saliva-coated 96-well microtiter plates (Figure 3) [21]. Because the biofilm occupied the full space of wells in conditions without butyric acid, the action of butyric acid to further upregulate biofilm formation is unknown. Therefore, SCFAs may not have

upregulated the biofilm in our study because of a physical limitation. Metabolites including lactic acid during cell growth were naturally produced and accumulated in TSBs with SCFAs, and the mixture of metabolites and exogenous SCFAs stresses biofilm cells in 96-well culture plates (Figure 4). Therefore, dead cells might be induced as a stress response in the biofilm, and the mixture of metabolites caused more damages to biofilm cells in 96-well culture plates than in the flow cell system. However, in the flow cell system without metabolite produced during growth, 6.25 mM butyric acid induced more damaged cells than no butyric acid (Figure 5). Extra-cellular DNA (eDNA) is released from dead cells and serves important functions as a factor of attachment to surfaces and an adhesive factor for bacteria during the initial stage of biofilm formation [30,31]. Butyric acid may exhibit biological activities similar to the release of eDNA and lead to biofilm formation.

Type 1 fimbriae mediate binding to N-acetyl-beta-D-galactosamine, PRPs and statherin, and these fimbriae are more common on *A. naeslundii* genospecies 2 (an early plaque colonizer) than genospecies 1 (a late plaque colonizer) [32, 33]. Type 2 fimbriae mediate binding to β-linked galactose and galactosamine structures, and these fimbriae are highly prevalent on *A. naeslundii* genospecies 1 and 2. FimA is a type 2 fimbriae that is a very important factor for *A. oris* biofilm formation. FimA did not contribute to 6h biofilm formation, but largely contributed to 16 h biofilm formation on the human saliva-coated 96-well microtiter plates in the present

study (Figure 2 and Figure 3). This result is consistent with the association of FimA with late biofilm development in *A. oris* [34–36]. Butyric acid, propionic acid and valeric acid inhibited MG1 and MG1.Δ*fimA* biofilm formation for 6 and 16 h in human saliva-coated 96-well microtiter plates. Therefore, the inhibitory effects of high concentrations of SCFAs are likely independent of FimA. A flow cell system was also used to remove the influence of these metabolites during growth and to examine the pure effects of exogenous SCFAs on *A. oris* MG1 and MG1.Δ*fimA* biofilm formation. Notably, 6.25 mM butyric acid and 3.125 mM propionic acid increased biofilms that included dead *A. oris* MG1 cells, but did not increase the biofilm of MG1.Δ*fimA* in the flow cell system. These data suggest that in in vitro experimental systems, 6.25 mM butyric acid and 3.125 mM propionic acid promote dead cells in FimA-dependent biofilm formation, and in dead cells, cell contents leak out and inherently make the cells stick more to each other, enhancing the appearance of the biofilm. This may link the function of FimA to *A. oris* biofilm formation.

It is known that CSP-mediated regulation is associated with biofilm formation of *S. mutans*. However, *SMU.940* gene was not identified as competence genes in previous studies [51-55]. Therefore, biofilm formation of *SMU.940* mutant was compared with that of parental strain. The aggregation and biofilm formation of the *SMU.940* mutant was distinct from parental strain. It was found that the *SMU.940* gene played a role in early biofilm formation; therefore,

the mechanism of *SMU.940*-dependent biofilm formation was investigated.

The mechanism and ecological significance of the dextran-dependent bacterial aggregation are subject to speculation. Dextran-dependent aggregation is related to the growth medium. This phenotype has been observed only in a semi-rich medium containing glucose and was absent in cultures grown in rich media, such as Todd-Hewitt or BHI broth [46]. In addition, the induction of aggregation required the presence of dextran and a stressor, including sub-lethal concentrations of antibiotics, ethanol, or xylitol, as previously reported [46, 50]. We also found that neither the *S. mutans* UA159 parental strain nor the derivative *SMU.940* mutant aggregated when grown in Todd-Hewitt or BHI, even in the presence of exogenously added dextran or a stressor (data not shown). Furthermore, we determined that TSB with 0.25% glucose (i.e. semi-rich medium) induced strong aggregation in the presence of ethanol, and the parental strain exhibited more dextran-dependent aggregation in the presence of ethanol and dextran than that in the presence of ethanol alone. The mechanisms of this dextran-dependency are currently unknown. The dextran-dependent aggregation has been attributed to GbpC [46]. These data showed that the inactivation of *gbpC* completely prevented the aggregation of the *SMU.940* mutant. This finding suggests that the rapid aggregation of the *SMU.940* mutant may be caused by GbpC.

In conclusion, in flow cell systems, 6.25 mM butyric acid and 3.13 mM propionic acid

promoted dead cells in FimA-dependent biofilm formation and increased attached and aggregated dead cells. These results indicate that SCFAs from other oral bacteria, such *P. gingivalis* and *F. nucleatum*, stimulated FimA-dependent biofilm formation of *A. oris*, which is involved in stress responses. However, the metabolites produced during cell growth disturbed the SCFA-induced FimA-dependent biofilm formation. This study did not elucidate the molecules involved in biofilm formation mechanisms. Further studies of the relationship between FimA and SCFAs are necessary to fully understand *A. oris* biofilm formation. To our knowledge, the present study is the first report of an effect of SCFAs on FimA in the in vitro biofilm formation of *A. oris*. On the other hands, it was demonstrated that a mutation in the *SMU.940* gene induced dextran-dependent rapid aggregation and early biofilm formation in TSB with 0.25% glucose and slightly reduced biofilm formation in TSB with 0.25% sucrose. These data indicate that *SMU.940* regulates the expression of GbpC, aggregation and, subsequently, biofilm formation in *S. mutans*.

**References**

1. Kolenbrander, P.E.; Palmer, R.J., Jr.; Periasamy, S.; Jakubovics, N.S. Oral multispecies biofilm development and the key role of cell-cell distance. Nat. Rev. Microbiol. 2010, 8, 471–480.

2. Nyvad, B.; Kilian, M. Microbiology of the early colonization of human enamel and root surfaces in vivo. Scand. J. Dent. Res. 1987, 95, 369–380.

3. Al-Ahmad, A.; Wunder, A.; Auschill, T.M.; Follo, M.; Braun, G.; Hellwig, E.; Arweiler, N.B. The in vivo dynamics of *Streptococcus* spp., *Actinomyces naeslundii*, *Fusobacterium nucleatum* and *Veillonella* spp. in dental plaque biofilm as analysed by five-colour multiplex fluorescence in situ hybridization. J. Med. Microbiol. 2007, 56, 681–687.

4. Do, T.; Henssge, U.; Gilbert, S.C.; Clark, D.; Beighton, D. Evidence for recombination between a sialidase (nanH) of *Actinomyces naeslundii* and *Actinomyces oris*, previously named '*Actinomyces naeslundii* genospecies 1 and 2'. FEMS Microbiol. Lett. 2008, 288, 156–162.

5. Henssge, U.; Do, T.; Gilbert, S.C.; Cox, S.; Clark, D.; Wickstom, C.; Ligtenberg, A.J.M.; Radford, D.R.; Beighton, D. Application of MLST and pilus gene sequence comparisons to investigate the population structures of *Actinomyces naeslundii* and *Actinomyces oris*. PLoS ONE 2009, 6, 21430–21441.

6. Paddick, J.S.; Brailsford, S.R.; Kidd, E.A.; Gilbert, S.C.; Clark, D.T.; Alam, S.; Killick, Z.J.;

Beighton, D. Effect of the environment on genotypic diversity of *Actinomyces naeslundii* and *Streptococcus oralis* in the oral biofilm. Appl. Environ. Microbiol. 2003, 69, 6475–6480.

7. Yeung, M.K.; Ragsdale, P.A. Synthesis and function of *Actinomyces naeslundii* T14V Type 1 fimbriae require the expression of additional fimbria-associated genes. Infect. Immun. 1997, 65, 2629–2639.

8. Arai, T.; Ochiai, K.; Senpuku, H. *Actinomyces naeslundii* GroEL-dependent initial attachment and biofilm formation in a flow cell system. J. Microbiol. Methods 2015, 109, 160–166.

9. Burne, R.A. Oral streptococci... products of their environment. J. Dent. Res. 1998, 77, 445–452.

10. Desaymard, C.; Ivanyi, L. Comparison of in vitro immunogenicity, tolerogenicity and mitogenicity of dinitrophenyl-levan conjugates with varying epitope density. Immunology 1976, 30, 647–653.

11. Shilo, M.; Wolman, B. Activities of bacterial levans and of lipopolysaccharides in the processes of inflammation and infection. Br. J. Exp. Pathol. 1958, 39, 652–660.

12. Mishra, A.; Das, A.; Cisar. J.O.; Ton-That, H. Sortase-catalyzed assembly of distinct heteromeric fimbriae in *Actinomyces naeslundii*. J. Bacteriol. 2007, 189, 3156–3165.

13. Wu, C.; Mishra, A.; Yang, J.; Cisar, J.O.; Das, A.; Ton-That, H. Dual function of a tip fimbrillin of *Actinomyces* in fimbrial assembly and receptor binding. J. Bacteriol. 2011, 193,

3197–3206.

14. Mishra, A.; Wu, C.; Yang, J.; Cisar, J.O.; Das, A.; Ton-That, H. The type 2 fimbrial shaft FimA mediates co-aggregation with oral streptococci, adherence to red blood cells and biofilm development. Mol. Microbiol. 2010, 77, 841–854.

15. Cisar, J.O.; Curl, S.H.; Kolenbrander, P.E.; Vatter, A.E. Specific absence of type 2 fimbriae on a coaggregation-defective mutant of *Actinomyces viscosus* T14V. Infect. Immun. 1983, 40, 759–765.

16. McIntire, F.C.; Crosby, L.K.; Vatter, A.E.; Cisar, J.O.; McNeil, M.R.; Bush, C.A.; Tjoa, S.S.; Fennessey, P.V. A polysaccharide from *Streptococcus sanguis* 34 that inhibits coaggregation of *S. sanguis* 34 with *Actinomyces viscosus* T14V. J. Bacteriol. 1988, 170, 2229–2235.

17. Niederman, R.; Buyle-Bodin, Y.; Lu, B.Y.; Robinson, P.; Naleway, C. Short-chain carboxylic acid concentration in human gingival crevicular fluid. J. Dent. Res. 1997, 76, 575–579.

18. Bendyk, A.; Marino, V.; Zilm, P.S.; Howe, P.; Bafold, P.M. Effect of dietary omega-3 polyunsaturated fatty acids on experimental periodontitis in the mouse. J. Periodontal. Res. 2009, 44, 211–216.

19. Yoo, S.; Geum-Sun, A. Correlation of microorganisms and carboxylic acid in oral cavity. Int. J. Clin. Prev. Dent. 2015, 11, 165–170.

20. Margolis, H.C.; Duckworth, J.H.; Moreno, E.C. Composition and buffer capacity of pooled

starved plaque fluid from caries-free and caries-susceptible individuals. J. Dent. Res. 1988, 67, 1476–1482.

21. Yoneda, S.; Kawarai, T.; Narisawa, N.; Tuna, E.B.; Sato, N.; Tsugane, T.; Saeki, Y.; Ochiai, K.; Senpuku, H. Effects of short-chain fatty acids on *Actinomyces naeslundii* biofilm formation. Mol. Oral Microbiol. 2013, 28, 354–365.

22. Motegi, M.; Takagi, Y.; Yonezawa, H.; Hanada, N.; Terajima, J.; Watanabe, H.; Senpuku, H. Assessment of genes associated with *Streptococcus mutans* biofilm morphology. Appl. Environ. Microbiol. 2016, 72, 6277–6287.

23. Gibbons, R.J.; Hay, D.I.; Cisar, J.O.; Clark, W.B. Adsorbed salivary proline-rich protein 1 and statherin: Receptors for type 1 fimbriae of *Actinomyces viscosus* T14V-J1 on apatitic surfaces. Infect. Immun. 1988, 56, 2990–2993.

24. Li, T.; Khah, M.K.; Slavnic, S.; Johansson, I.; Strömberg, N. Different type 1 fimbrial genes and tropisms of commensal and potentially pathogenic *Actinomyces* spp. with different salivary acidic proline-rich protein and statherin ligand specificities. Infect. Immun. 2001, 69, 7224–7233.

25. Ruhl, S.; Sandberg, A.L.; Cisar, J.O. Salivary receptors for the proline-rich protein-binding and lectin-like adhesins of oral *Actinomyces* and *Streptococci*. J. Dent. Res. 2004, 83, 505–510.

26. Palmer, R.J., Jr.; Gordon, S.M.; Cisar, J.O.; Kolenbrander, P.E. Coaggregation-mediated

interactions of *Streptococci* and *Actinomyces* detected in initial human dental plaque. J. Bacteriol. 2003, 185, 3400–3409.

27. Bergeron, L.J.; Burne, R.A. Roles of fructosyltransferase and levanase-sucrase of *Actinomyces naeslundii* in fructan and sucrose metabolism. Infect. Immun. 2001, 69, 5395–5402.

28. Thurnheer, T.; Guggenheim, B.; Gmür, R. Characterization of monoclonal antibodies for rapid identification of *Actinomyces naeslundii* in clinical samples. FEMS Microbiol. Lett. 1997, 150, 255–262.

29. Bowden, G.H.; Nolette, N.; Ryding, H.; Cleghorn, B.M. The diversity and distribution of the predominant ribotypes of *Actinomyces naeslundii* genospecies 1 and 2 in samples from enamel and from healthy and carious root surfaces of teeth. J. Dent. Res. 1999, 78, 1800–1809.

30. Das, T.; Sharma, P.K.; Busscher, H.J.; van der Mei, H.C.; Krom, B.P. Role of extracellular DNA in initial bacterial adhesion and surface aggregation. Appl. Environ. Microbiol. 2010, 76, 3405–3408.

31. Das, T.; Sehar, S.; Manefield, M. The roles of extracellular DNA in the structural integrity of extracellular polymeric substance and bacterial biofilm development. Environ. Microbiol. Rep. 2013, 5, 778–786.

32. Hallberg, K.; Hammarström, K.-J.; Falsen, E.; Dahlen, G.; Gibbons, R.; Hay, D.I.;

Strömberg, N. *Actinomyces naeslundii* genospecies 1 and 2 express different binding specificities to N-acetyl-β-D-galactosamine, whereas *Actinomyces odontolyticus* expresses a different binding specificity in colonizing the human mouth. Oral Microbiol. Immunol. 1998, 13, 327–336.

33. Hallberg, K.; Holm, C.; Öhman, U.; Strömberg, N. *Actinomyces naeslundii* displays variant fimP and fimA fimbrial subunit genes corresponding to different types of acidic proline-rich protein and beta-linked galactosamine binding specificity. Infect. Immun. 1998, 66, 4403–4410.

34. Cisar, J.O.; Sandberg, A.L.; Mergenhagen, S.E. Lectin-dependent attachment of *Actinomyces naeslundii* to receptors on epithelial cells. Infect. Immun. 1984, 46, 459–464.

35. Cisar, J.O.; Vatter, A.E.; Clark, W.B.; Curl, S.H.; Hurst-Calderone, S.; Sandberg, A.L. Mutants of *Actinomyces viscosus* T14V lacking type 1, type 2, or both types of fimbriae. Infect. Immun. 1988, 56, 2984–2989.

36. Whittaker, C.J.; Klier, C.M.; Kolenbrander, P.E. Mechanisms of adhesion by oral bacteria. Annu. Rev. Microbiol. 1996, 50, 513–552.

37. Mitchell TJ. The pathogenesis of streptococcal infections: from tooth decay to meningitis. Nat Rev Microbiol. 2003;1:219-230.

38. Kuramitsu HK, He X, Lux R, Anderson MH, Shi W. Interspecies interactions within oral microbial communities. Microbiol Mol Biol Rev. 2007;71:653-670.

39. Munro CL, Michalek SM, Macrina FL. Sucrose-derived exopolymers have site-dependent roles in *Streptococcus mutans*-promoted dental decay. FEMS Microbiol Lett. 1995;128:327-332.

40. Yamashita Y, Bowen WH, Burne RA, Kuramitsu HK. Role of the *Streptococcus mutans gtf* genes in caries induction in the specific-pathogen-free rat model. Infect Immun. 1993;61:3811-3817.

41. Aoki H, Shiroza T, Hayakawa M, Sato S, Kuramitsu HK. Cloning of a *Streptococcus mutans* glucosyltransferase gene coding for insoluble glucan synthesis. Infect Immun. 1986;53:587-594.

42. Lynch DJ, Fountain TL, Mazurkeiwicz JE, Banas JA. Glucan-binding proteins are essential for shaping *Streptococcus mutans* biofilm architecture. FEMS Microbiol Lett. 2007;268:158-165.

43. Duque C, Stipp RN, Wang B, et al. Downregulation of GbpB, a component of the VicRK regulon, affects biofilm formation and cell surface characteristics of *Streptococcus mutans*. Infect Immun. 2011;79:786-796.

44. Matsumura M, Izumi T, Matsumoto M, et al. The role of glucan-binding proteins in the cariogenicity of *Streptococcus mutans*. Microbiol Immunol. 2003;47:213-215.

45. Matsumoto M, Fujita K. Ooshima T et al. Binding of glucan-binding protein C to GTFD-synthesized soluble glucan in sucrose-dependent adhesion of *Streptococcus mutans*. Oral

Microbiol Immunol. 2006;21:42-46.

46. Sato Y, Yamamoto Y, Kizaki H. Cloning and sequence analysis of the *gbpC* gene encoding a novel glucan-binding protein of *Streptococcus mutans*. Infect Immun. 1997;65:668-675.

47. Takashima Y, Fujita K, Ardin AC, et al. Characterization of the dextran-binding domain in the glucan-binding protein C of *Streptococcus mutans*. J Appl Microbiol. 2015;119:1148-1157.

48. Sato Y, Senpuku H, Okamoto K, Hanada N, Kizaki H. *Streptococcus mutans* binding to solid phase dextran mediated by the glucan-binding protein C. Oral Microbiol Immunol. 2002;17:252-256.

49. Motegi M, Takagi Y, Yonezawa H, et al. Assessment of genes associated with *Streptococcus mutans* biofilm morphology. Appl Environ Microbiol. 2006;72:6277-6287.

50. Sato Y, Yamamoto Y, Kizaki H. Xylitol-induced elevated expression of the *gbpC* gene in a population of *Streptococcus mutans* cells. Eur J Oral Sci. 2000;108:538-545.

51. Reck M, Tomasch J, Wagner-Döbler I. The alternative sigma factor SigX controls bacteriocin synthesis and competence, the two quorum sensing regulated traits in *Streptococcus mutans*. PLoS Genet. 2015;11:e1005353.

52. Lemme A, Gröbe L, Reck M, Tomasch J, Wagner-Döbler I. Subpopulation-specific transcriptome analysis of competence-stimulating-peptide-induced *Streptococcus mutans*. J Bacteriol. 2011;193:1863-1877.

53. Perry JA, Jones MB, Peterson SN, Cvitkovitch DG, Lévesque CM. Peptide alarmone signalling triggers an auto-active bacteriocin necessary for genetic competence. Mol Microbiol. 2009;72:905-917.

54. Dufour D, Cordova M, Cvitkovitch DG, Lévesque CM. Regulation of the competence pathway as a novel role associated with a streptococcal bacteriocin. J Bacteriol. 2011;193:6552-6559.

55. Okinaga T, Niu G, Xie Z, Qi F, Merritt J. The hdrRM operon of *Streptococcus mutans* encodes a novel regulatory system for coordinated competence development and bacteriocin production. J Bacteriol. 2010;192:1844-1852.

**Figure legends**

Figure 1. Effect of SCFAs on biofilm formation for 6 h in human saliva-coated and non-coated plates.

Effects of 6.25-30 mM butyric acid (A), propionic acid (B) and valeric acid (C) on *A. oris* MG1 biofilm formation for 6 h in human saliva-coated and non-coated 96-well microtiter plates. The data show the mean ± standard deviation (SD) of three independent assays. The asterisks indicate a significant difference between multiple groups (one-way analysis of variance and post-hoc Turkey's test: * $p < 0.05$, control: no SCFA vs. concentrations of SCFA) and the two groups (Student's t-test: ** $p < 0.05$, control: no coating vs. saliva-coating).

Figure 2. Effects of SCFAs on *A. oris* MG1 and MG1.Δ*fimA* biofilm formation for 6 h in human saliva-coated plates.

Effects of 6.25-30 mM butyric acid (A), propionic acid (B) and valeric acid (C) on *A. oris* MG1 and MG1.Δ*fimA* biofilm formation for 6 h in human saliva-coated 96-well microtiter plates. The data show the mean ± standard deviation (SD) of three independent assays. The asterisks indicate a significant difference between multiple groups (one-way analysis of variance and post-hoc Turkey's test: * $p < 0.05$, control: no SCFA vs. concentrations of SCFA).

Figure 3. Effects of SCFAs on *A. oris* MG1 and MG1.Δ*fimA* biofilm formation for 16 h in human saliva-coated plates.

Effects of 3.125–60 mM butyric acid (A), propionic acid (B) and valeric acid (C) on *A. oris* MG1 and MG1.Δ*fimA* biofilm formation for 16 h in human saliva-coated 96-well microtiter plates. The data show the mean ± standard deviation (SD) of three independent assays. The asterisks indicate a significant difference between the two groups (Student's t-test: * $p < 0.05$, MG1 vs. MG1.Δ*fimA*).

Figure 4. Effects of 6.25 mM butyric acid on *A. oris* MG1 and MG1.Δ*fimA* biofilm formation for 16 h on human saliva-coated cover glass in six-well microtiter plates.

Effects of 6.25 mM butyric acid on *A. oris* MG1 and MG1.Δ*fimA* biofilm formation were observed on human saliva-coated cover glass in six-well microtiter plates. *A. oris* biofilms were stained using a LIVE/DEAD BacLight viability kit and analyzed using a confocal microscope and Zen software. Live and dead cells are indicated with green and red colors, respectively. Live (left), dead (center) and merged cells (right) are present in biofilm stimulated with or without butyric acid. Representative data from more than three independent experiments are presented in the pictures.

Figure 5. Effects of 6.25 mM butyric acid on *A. oris* MG1 and MG1.Δ*fimA* biofilm formation for 48 h in a flow cell system.

Effects of 6.25 mM butyric acid on *A. oris* MG1 and MG1.Δ*fimA* biofilm formation were observed in a flow cell system. *A. oris* biofilms were stained using a LIVE/DEAD BacLight viability kit and analyzed using a confocal microscope and Zen software. Live and dead cells are indicated with green and red colors, respectively. Live (left), dead (center) and merged cells (right) are presented in biofilms stimulated with or without butyric acid. Representative data from more than three independent experiments are presented in the pictures.

Figure 6. Visual analysis of the effect of butyric acid on biofilm formation of *A. oris* MG1 in a flow cell system.

Effects of 6.25 mM butyric acid on the biofilm formation of *A. oris* MG1 were observed and compared with no butyric acid in a flow cell system. The biofilm formation of *A. oris* was stained by a LIVE/DEAD BacLight viability kit and analyzed by confocal microscope and Zen software. Live and dead cells were indicated as green and red color cells, respectively. X-Y and X-Z axis are presented in biofilm stimulated with no butyric acid and butyric acid. Representative data from more than three independent experiments are presented in the picture.

Figure 7. Effects of 3.125 mM propionic acid on *A. oris* MG1 and MG1.Δ*fimA* biofilm formation for 48 h in a flow cell system.

Effects of 3.125 mM propionic acid on *A. oris* MG1 and MG1.Δ*fimA* biofilm formation were observed in a flow cell system. *A. oris* biofilms were stained using a LIVE/DEAD BacLight viability kit and analyzed using a confocal microscope and Zen software. Live and dead cells are indicated with green and red colors, respectively. Live (left), dead (center) and merged cells (right) are presented in biofilms stimulated with or without butyric acid. Representative data from more than three independent experiments are presented in the pictures.

Figure 8. Live and dead cells area ($mm^2$) for the effect of propionic acid on biofilm formation of *A. oris* MG1 in a flow cell system.

Images from Figure 7 were further analyzed as a mixture of live and dead cell areas ($mm^2$) using ImageJ. The data are represented as the mean ± standard deviation (SD) of images from three independent assays. The asterisks indicate a significant difference between the two groups (Student's t-test: *; $p < 0.05$, no SCFA vs. SCFA).

Figure 9. Biofilm formation by parental and mutant strains of *S. mutans*.

Quantification of biofilm biomass grown in tryptic soy broth without dextrose (TSB) with

0.25% glucose (A) or TSB with 0.25% sucrose (B). Cells were grown at 37°C for 8 h in 96-well polystyrene microtiter plates. The data are expressed as the mean ± standard deviation of three independent experiments (*P < .05).

Figure 10. Aggregation assay of wild-type, *SMU.940* mutant, *gbpC* mutant, and *SMU.940-gbpC* double mutant strains of *S. mutans*.

Each of the cultures was grown to mid-log phase in tryptic soy broth without dextrose (TSB) with 0.25% glucose without 4% ethanol (A and B) or overnight in TSB with 0.25% glucose and 4% ethanol (C and D). After centrifuging and re-suspending the bacteria in PBS, 100 μg/mL dextran was added to each culture (B and D). After growing overnight in TSB with 0.25% glucose, the degree of aggregation was evaluated by measuring the turbidity of the re-suspended cultures at 0, 5, 10, 15, 20, 25, 30, and 60 min by measuring the $OD_{620}$. The data are expressed as the mean ± standard deviation of three independent experiments. Representative photographs were taken after 5 min. Aggregation of the wild-type (WT) was observed under the ethanol and ethanol and dextran conditions but not under the condition without the addition of dextran. In contrast, the aggregation of the *SMU.940* mutant was observed, but the aggregations of the two *gbpC* mutant strains (*gbpC*− and *940-gbpC*−) were not observed under all conditions.

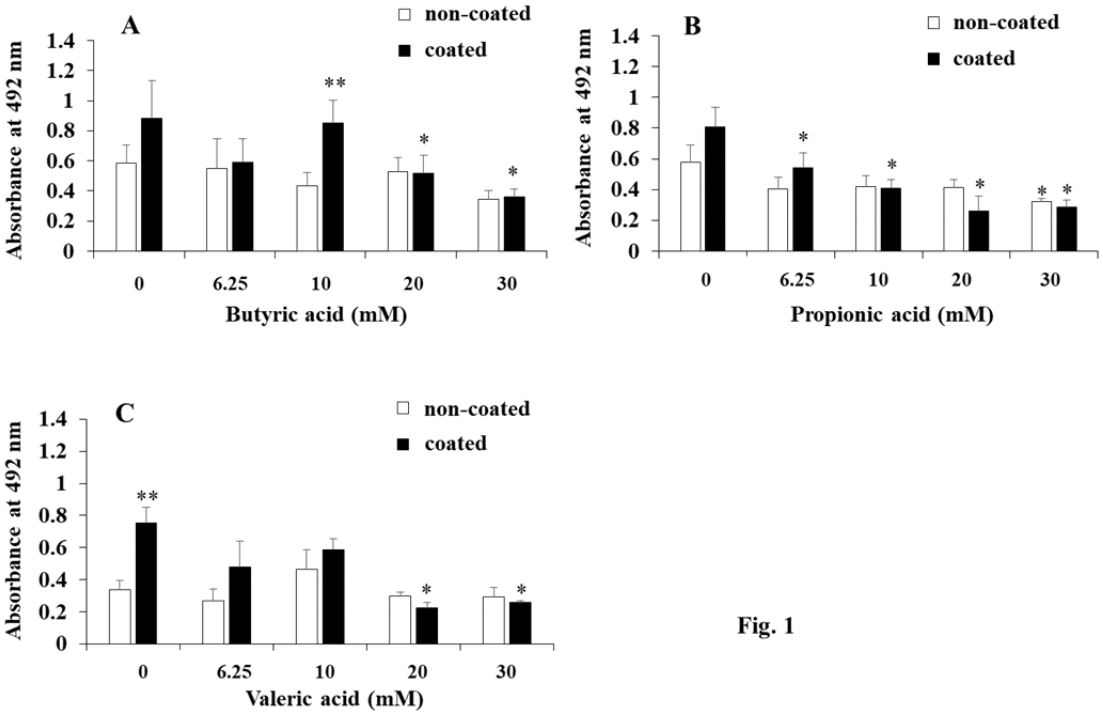
A
non-coated
coated
Absorbance at 492 nm
1.4
1.2
1
0.8
0.6
0.4
0.2
0
**
*
*
0
6.25
10
20
30
Butyric acid (mM)
B
non-coated
coated
Absorbance at 492 nm
*
*
*
*
*
Propionic acid (mM)
C
non-coated
coated
Absorbance at 492 nm
**
*
*
Valeric acid (mM)

**Fig. 1**

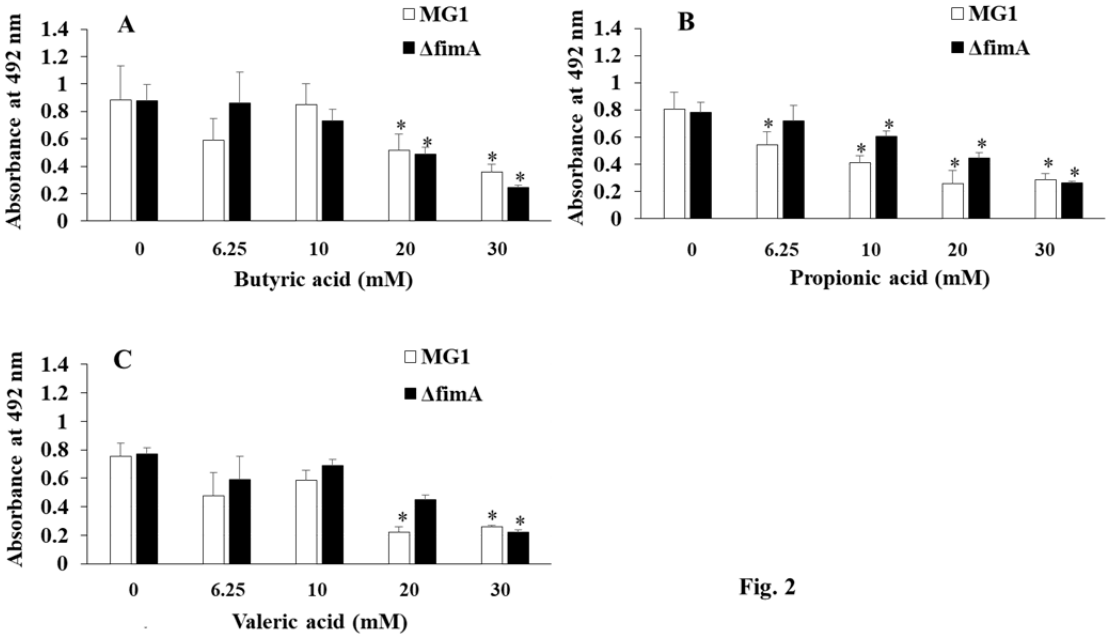
A
MG1
ΔfimA
Absorbance at 492 nm
1.4
1.2
1
0.8
0.6
0.4
0.2
0
0
6.25
10
20
30
Butyric acid (mM)
B
MG1
ΔfimA
Absorbance at 492 nm
Propionic acid (mM)
C
MG1
ΔfimA
Absorbance at 492 nm
Valeric acid (mM)

Fig. 2

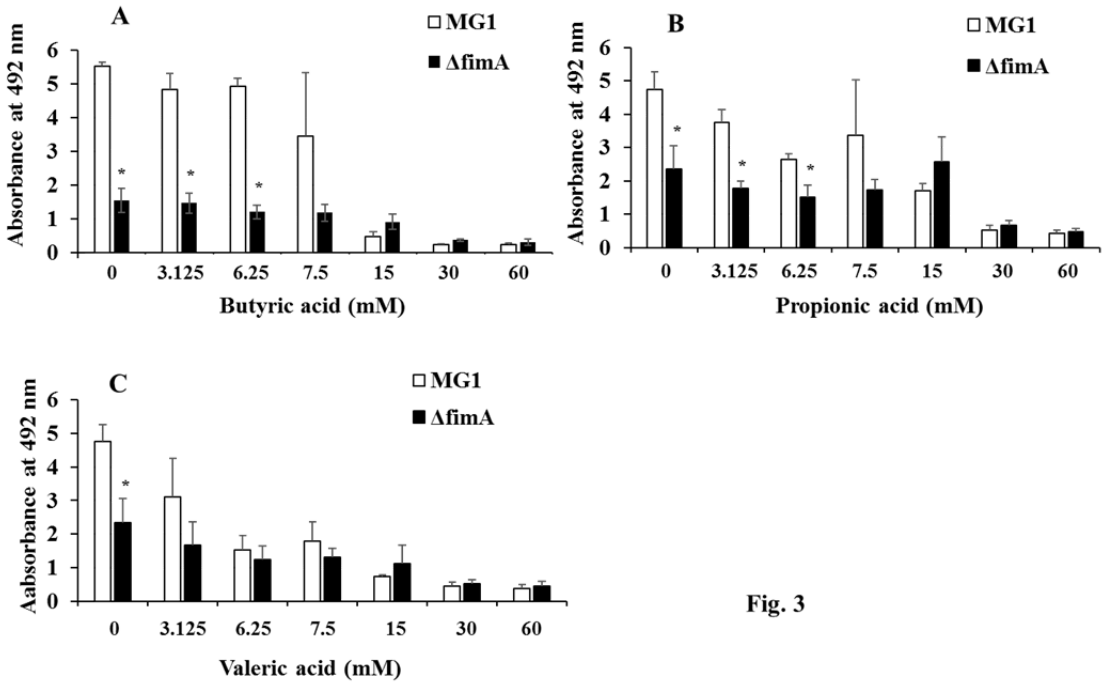
A
MG1
ΔfimA
Absorbance at 492 nm
0
1
2
3
4
5
6
*
0
3.125
6.25
7.5
15
30
60
Butyric acid (mM)
B
MG1
ΔfimA
Absorbance at 492 nm
*
*
*
0
3.125
6.25
7.5
15
30
60
Propionic acid (mM)
C
MG1
ΔfimA
Aabsorbance at 492 nm
*
0
3.125
6.25
7.5
15
30
60
Valeric acid (mM)

**Fig. 3**

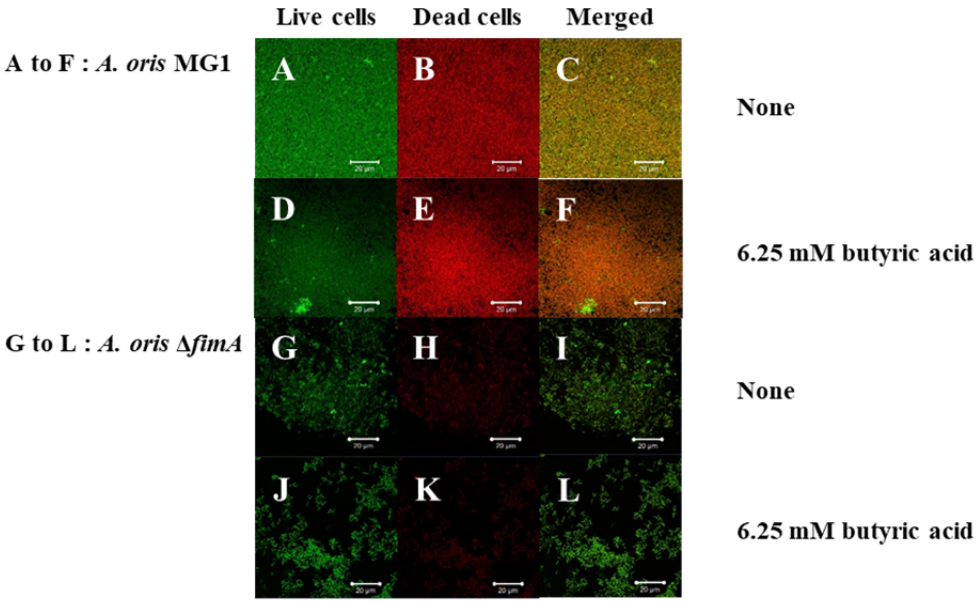
Live cells
Dead cells
Merged
A to F : A. oris MG1
A
B
C
None
D
E
F
6.25 mM butyric acid
G to L : A. oris ΔfimA
G
H
I
None
J
K
L
6.25 mM butyric acid

**Fig. 4**

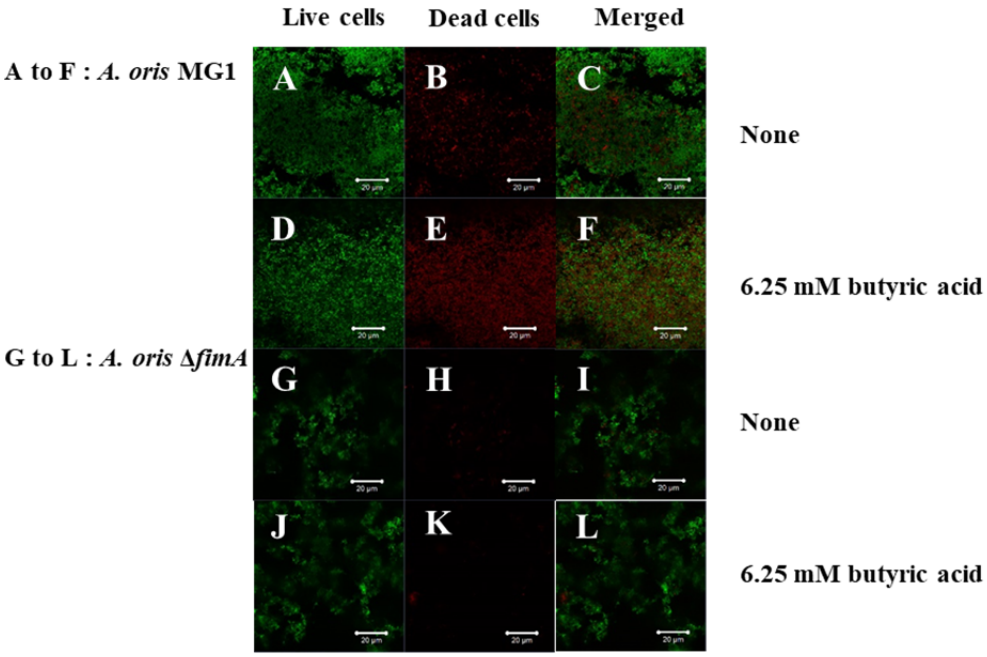
Live cells
Dead cells
Merged
A to F : A. oris MG1
G to L : A. oris ΔfimA
A
B
C
D
E
F
G
H
I
J
K
L
None
6.25 mM butyric acid
None
6.25 mM butyric acid

**Fig. 5**

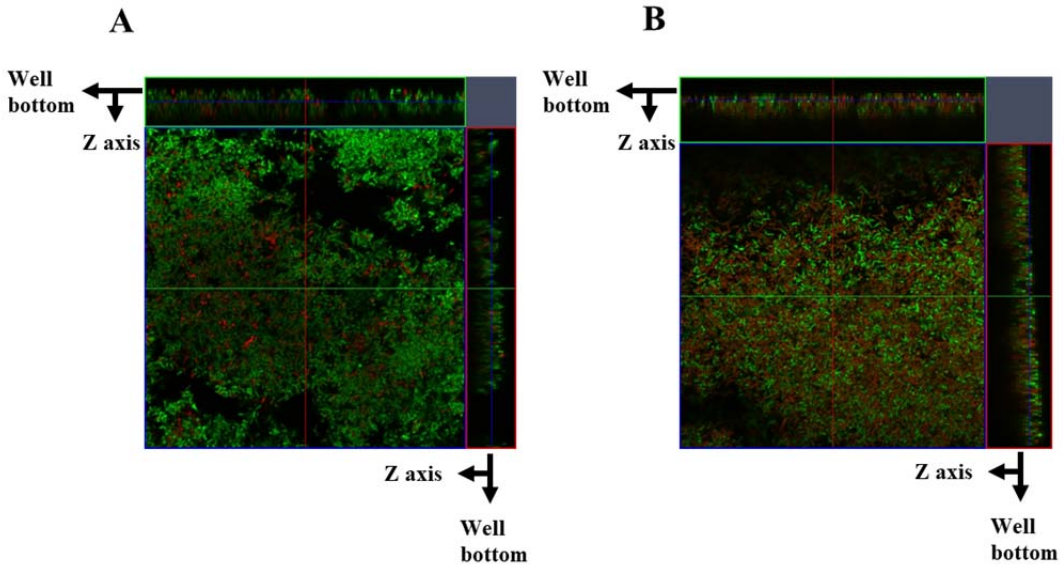


MG1 no butyric acid

MG1 +6.25 mM butyric acid

Fig. 6

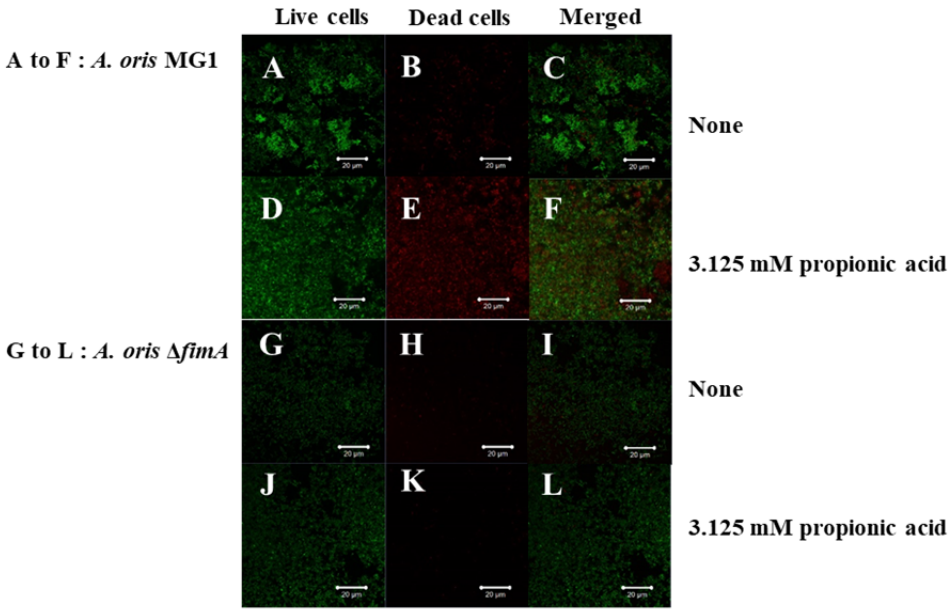
Live cells
Dead cells
Merged
A to F : A. oris MG1
A
B
C
None
D
E
F
3.125 mM propionic acid
G to L : A. oris ΔfimA
G
H
I
None
J
K
L
3.125 mM propionic acid

**Fig. 7**

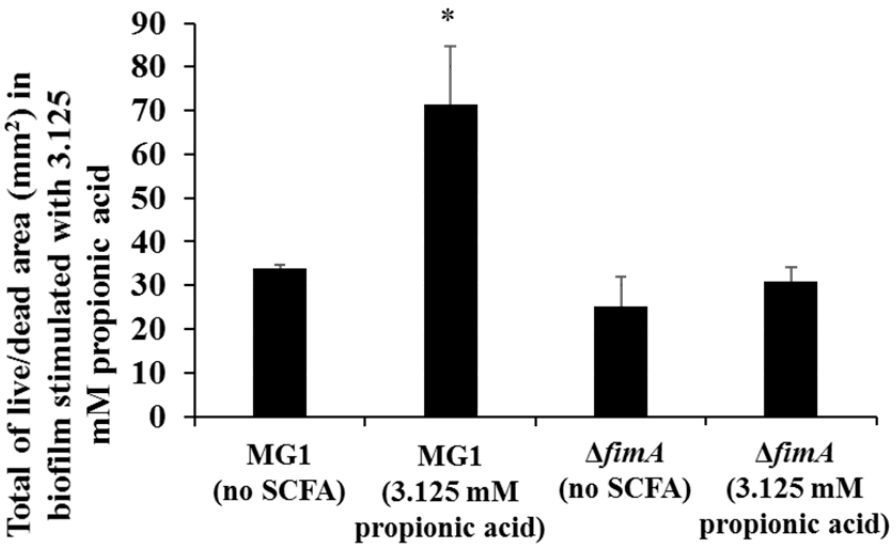
Total of live/dead area (mm²) in biofilm stimulated with 3.125 mM propionic acid
90
80
70
60
50
40
30
20
10
0
*
MG1 (no SCFA)
MG1 (3.125 mM propionic acid)
ΔfimA (no SCFA)
ΔfimA (3.125 mM propionic acid)

**Fig. 8**

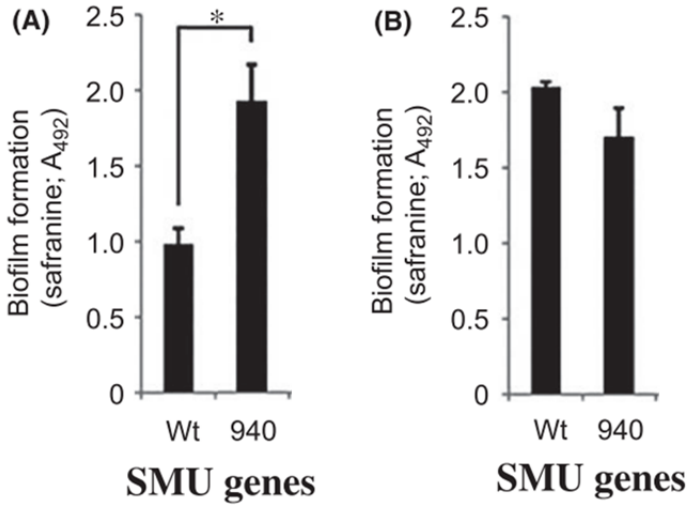
(A)
2.5
2.0
1.5
1.0
0.5
0
*
Biofilm formation (safranine; $A_{492}$)
Wt
940
SMU genes
(B)
2.5
2.0
1.5
1.0
0.5
0
Biofilm formation (safranine; $A_{492}$)
Wt
940
SMU genes

**Fig. 9**

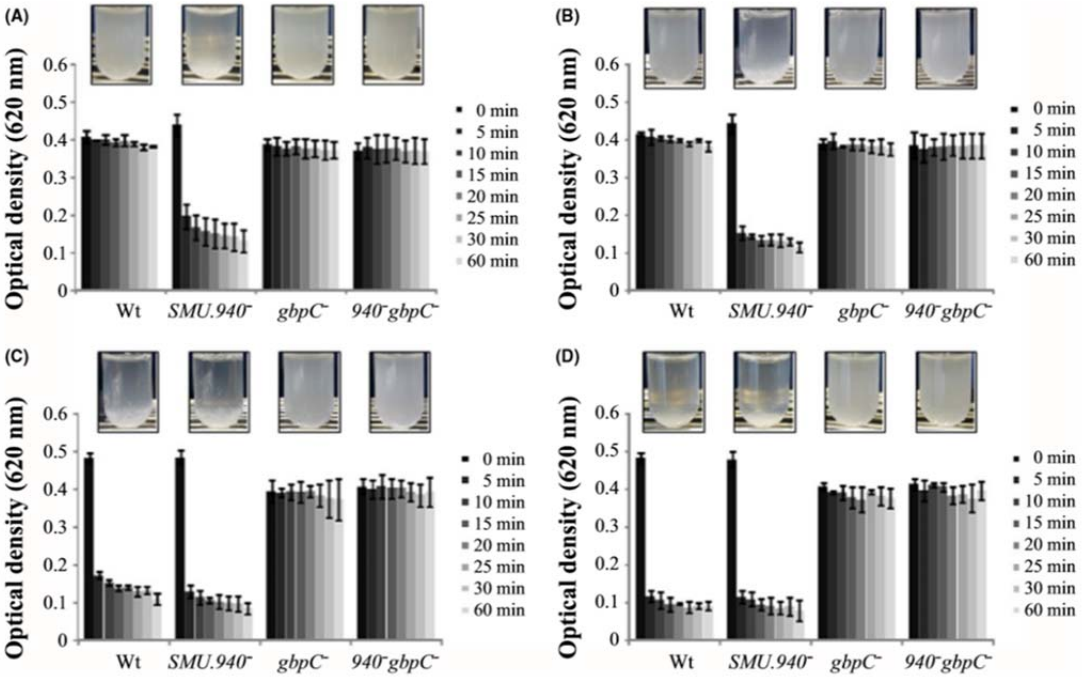
(A)
(B)
(C)
(D)
Optical density (620 nm)
0
0.1
0.2
0.3
0.4
0.5
0.6
Wt
SMU.940-
gbpC-
940-gbpC-
0 min
5 min
10 min
15 min
20 min
25 min
30 min
60 min

**Fig. 10**